

# A new window into cool dwarfs' magnetospheres: radiation belts and beyond

Climent, J. B.<sup>1</sup>, Guirado, J. C.<sup>1</sup>, Pérez-Torres, M.<sup>2,3</sup>, Peña-Moñino, L.<sup>2</sup>, and Marcaide, J. M.<sup>4</sup>

<sup>1</sup> Departament d'Astronomia i Astrofísica, Universitat de València, C. Dr. Moliner 50, E-46100 Burjassot, València, Spain

<sup>2</sup> Instituto de Astrofísica de Andalucía, Consejo Superior de Investigaciones Científicas (CSIC), Glorieta de la Astronomía s/n, E-18008, Granada, Spain.

<sup>3</sup> Facultad de Ciencias, Universidad de Zaragoza, E-50009 Zaragoza Spain.

<sup>4</sup> Real Academia de Ciencias Exactas, Físicas y Naturales de España, E-28004 Madrid, Spain.

## Abstract

We present new insights into the magnetospheres of ultracool dwarfs (UCDs) through VLBI observations, focusing on LSR J1835+3259. Observations reveal a structured magnetosphere with complex radio emission, potentially analogous to radiation belts in gas giants. High-resolution radio imaging identified bursts of left circularly polarized emission, interpreted as electron cyclotron maser instability (ECMI) from magnetic poles, while quiescent radiation suggests a stable radiation belt. Comparisons with gas giant models indicate that UCDs may host radiation belts and auroral processes similar to those of Jupiter, advancing our understanding of magnetic phenomena in substellar objects. These findings underscore the role of VLBI in unveiling the magnetic architectures of UCDs and their potential similarities to planetary magnetic fields.

## 1 Introduction

Ultracool dwarfs (UCDs), which are fully convective stellar or sub-stellar objects with spectral types of M7 and later, have intrigued astronomers since their unexpected radio emissions were first detected [1]. Collaborative research has since identified radio emissions at gigahertz frequencies in dozens of such objects, with unbiased surveys reporting a detection rate of about 10% [2]. Importantly, there have also been two successful detections at megahertz frequencies [3, 4].

Radio emissions from UCDs are generally classified into bursting and non-bursting components. The non-bursting component has been observed in all radio-emitting UCDs except the T6 dwarf WISEP J112254.73+255021.5 [5], while the bursting component appears only in some. The periodic bursts coincide with the UCD's rotation period and are highly circularly polarized. These features have long been attributed to the electron cyclotron maser instability (ECMI) [6]. The absence of periodic pulses in certain UCDs may be due to the directional nature of ECMI emissions or because observations did not cover a full rotation period. This behavior contrasts with the solar-like magnetic activity paradigm [7] and suggests a resemblance to auroral activities observed on planets [8]. The solar-like model relies on a sustained magnetic field driven by an internal dynamo and non-thermal heating of the upper atmosphere. In contrast, the auroral model involves large-scale, field-aligned current systems that accelerate electrons and ions toward the atmosphere, leading to auroral emissions [9].

The non-bursting radio emissions, which exhibit low to moderate circular polarization, are well explained by synchrotron or gyrosynchrotron mechanisms [10]. The precise origin of these emissions remains unconfirmed. The Güdel-Benz relation [12] shows an empirical correlation between coronal X-ray and non-bursting radio emissions from F-type to M-type dwarf stars. UCDs deviate from this relation, indicating that their coronae are not significantly heated magnetically and that their non-bursting radio emissions cannot originate solely from coronal processes involving stellar gyrosynchrotron mechanisms [8]. An example is LSR J1835+3259, which exhibits one of the faintest X-ray emission limits [13] yet shows clear detections of non-bursting radio emissions [14, 13, 11, 15, 16].

A compelling explanation that aligns with the stable magnetosphere required by the auroral model for bursting emissions is the presence of energetic electrons trapped in radiation belts, analogous to those of Jupiter [6, 8]. In our solar system, Jupiter's moon Io is a major plasma source contributing to the planet's radiation belts and supplies the electrons that power its main auroral oval. Similarly, terrestrial planets orbiting UCDs could create conditions conducive to sustaining radiation belts (manifested as non-bursting radio emissions) and aurorae (observed as periodic bursting radio emissions). This scenario could link both components of UCDs' radio emissions and supports the preliminary evidence of their interconnection [8]. Admittedly, the magnetic activity of the UCD itself could be enough to sustain radiation belts without the need of a companion. In any case, detecting non-bursting radio emissions originating beyond the chromosphere would, in this context, confirm the existence of radiation belts and extensive current systems responsible for auroral activities.

## 2 Resolving UCD's magnetospheres for the first time

On June 15, 2021, the European VLBI Network (EVN) was used to observe the brown dwarf LSR J1835+3259, classified as an M8.5 spectral type. This object, located approximately  $5.6885 \pm 0.0015$  parsecs from Earth, rotates swiftly, with a period of  $2.84140 \pm 0.00039$  hours [17]. The observations revealed a complex radio structure for this ultracool dwarf (UCD) (see Fig. 1), with radio emissions extending up to 3 milliarcseconds (mas), equivalent to 0.017 astronomical units or about 33 times the dwarf's stellar radius ( $R_*$ ).

During our observation, we captured two bursts of left circularly polarized (LCP) radio emission in the light curve at rotational phases  $f_1 = 0.38 \pm 0.02$  and  $f_2 = 1.33 \pm 0.02$ , with LCP flux densities of  $3.7 \pm 0.2$  and  $1.5 \pm 0.2$  millijansky (mJy), respectively (see left panel of Fig. 2). We interpret these bursts, which we call B1 and B2, as originating from electron cyclotron maser instability (ECMI) emission. The time separating the peaks of these bursts was measured at  $2.70 \pm 0.02$  hours, nearly matching the rotational period though not identical. The right circularly polarized (RCP) emission showed gradual variation, reaching its peak before the bursts, while the quiescent LCP and RCP flux densities remained nearly equal, as expected for a weakly polarized, non-bursting component of LSR J1835+3259's radio output.

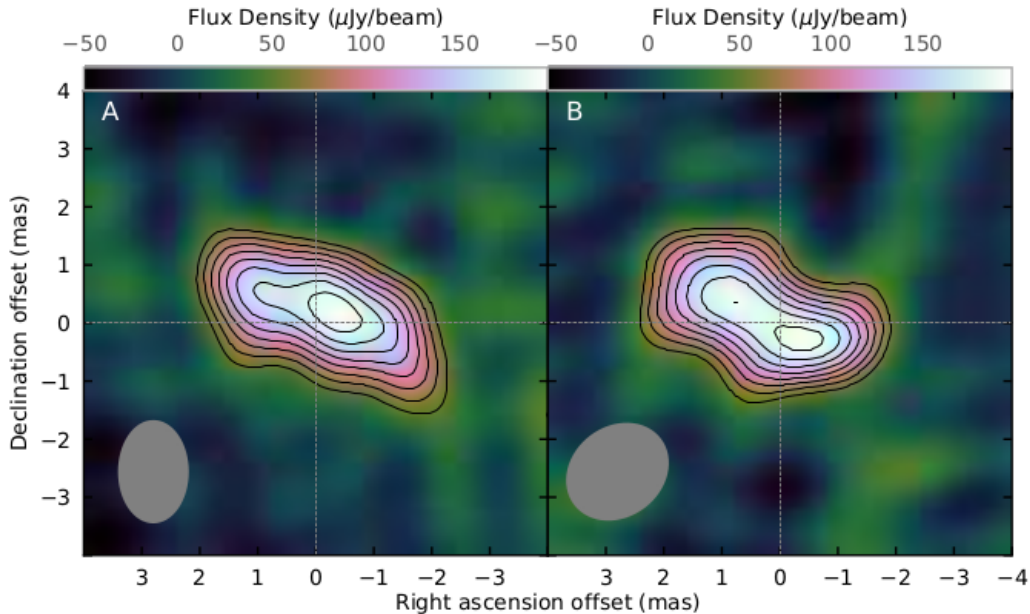


Figure 1: Reconstructed radio images of LSR J1835+3259 from the EVN observations on 15 June 2021 display Stokes I images during the first (A) and second (B) rotations. Contours show signal-to-noise ratios (S/N) from 3 upward, with detections at  $S/N \geq 5$ . Gray ellipses in the corners denote FWHM beam sizes, with dimensions of  $1.14 \times 1.70$  mas at  $0.0^\circ$  and  $1.49 \times 1.81$  mas at  $-53.9^\circ$ . The photosphere shift during the observing time was corrected. Both images are centered at the expected position of the optical photosphere, derived from optical astrometry. Credit: [18].

For burst B1 (rotation phase interval:  $0.29 < \phi < 0.47$ ), we generated images of the radio emission from LSR J1835+3259 (see right panel of Fig. 2). These images revealed that the steady, non-bursting radio component (characterized by total intensity or Stokes I parameter) resolved spatially into two distinct radio sources separated by  $2.3 \pm 0.2$  mas along an east-west axis, both showing minimal polarization (circular polarization  $< 10\%$ ). In contrast, the ECMI bursting component, traced by circular polarization (Stokes V parameter), appeared nearly centered between the two quiescent sources. During burst B2, a similar pattern was observed, but with the separation between the two sources reduced to approximately  $1.2 \pm 0.2$

mas, about half of what was observed in the first burst.

These radio images suggest a structure indicative of a radiation belt, with the observed emissions corresponding to energetic particles trapped along the brown dwarf’s magnetic field. This field likely has a dipolar configuration, as the ECMI emission is seen near the magnetic poles, and the detected double-lobed structure aligns with emissions typically produced by synchrotron radiation in radiation belts. This arrangement resembles Jupiter’s magnetic field and radiation belt configuration.

Comparing these observations with models, the findings suggest that LSR J1835+3259’s magnetosphere behaves similarly to those of gas giants, with energetic particles accelerated by magnetic reconnection. This process produces nonthermal gyrosynchrotron and synchrotron emission along magnetic lines and coherent ECMI emissions at the poles [18]. These similarities imply that UCDs with strong magnetic fields could have radiation belts and auroral emissions similar to those of planets like Jupiter.

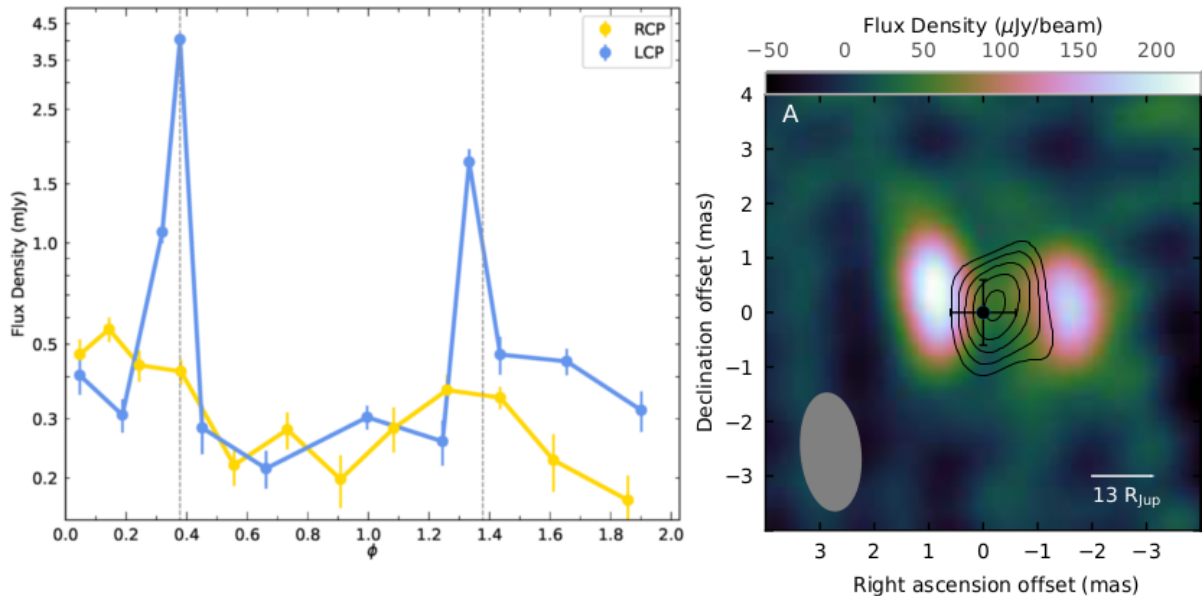


Figure 2: Left panel: Light curves of the radio emission from LSR J1835+3259 during the observations. Data points are RCP (yellow) and LCP (blue) flux densities of LSR J1835+3259. The two vertical dashed lines are separated by the rotation period of the object and use the first burst as the reference phase. Error bars indicate  $1\sigma$  uncertainties in the flux densities. Right panel: Reconstructed images of LSR J1835+3259 during the first radio burst. This image represents a 30-minute interval around bursts B1. To create the Stokes I images (color), we subtracted 10 minutes of LCP data centered on the burst peak. Black contours indicate Stokes V data for each 10-minute interval surrounding each burst, showing signal-to-noise ratios of 5, 6, 7, 8, and 9. The black dot marks the estimated size and position of the optical photosphere based on optical astrometry, with error bars representing the standard deviation from our astrometric analysis.

### 3 Other UCDs with VLBI

Beyond LSR J1835+3259, we have observed a small sample of UCDs with the VLBI technique. One of them is WISE J112254.72+255022.2 (hereafter J1122), a T6-type brown dwarf located at 15.9 pc. The radio emission of this UCD was initially detected at GHz frequencies using the Arecibo telescope [2], with further confirmation by the VLA [5]. Both instruments observed periodic radio bursts, though they reported different rotation periods: 17.3 minutes from pulsar timing at Arecibo and 116 minutes from the VLA lightcurve.

With the use of the Very Long Baseline Array (VLBA), we detected highly circularly polarised radio emission at the expected position of J1122, at 5 GHz in a series of 5 observations [19]. A Lomb-Scargle periodogram of the lightcurves reveals a signal at  $1.95 \pm 0.03$  hr, coinciding with the measurement of previous VLA observations [5] and thus discarding the 17.3 minute value reported using the Arecibo telescope. Remarkably, the phase-folded average lightcurve of the 5 epochs reveals a behavior well-predicted by an auroral ring model (see left panel of Fig. 3). In this model, ECMI emission arises from auroral rings at specific magnetic latitudes in both the northern and southern regions, similar to what is seen on Jupiter. However, due to emission beaming, only certain field lines within these rings will be visible to an observer at any given moment (see right panel of Fig. 3).

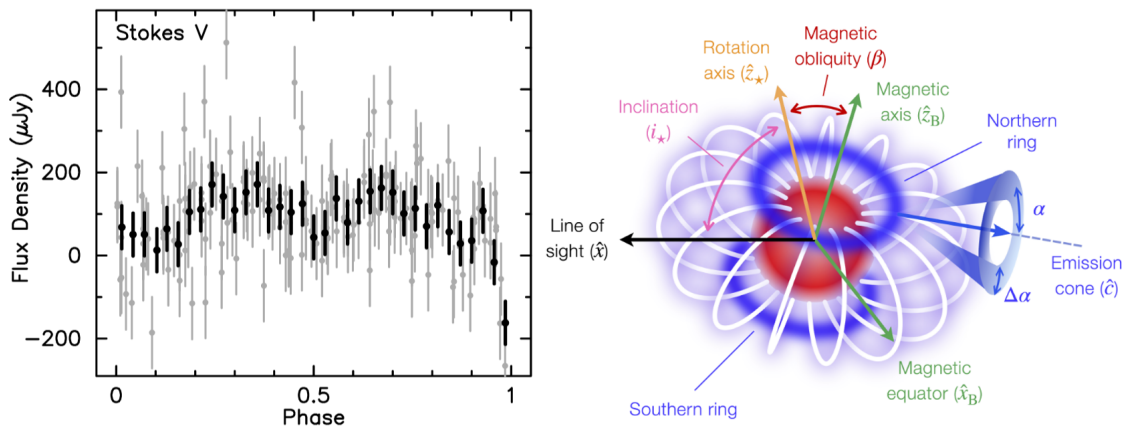


Figure 3: Left panel: Stokes V, phase-folded lightcurve of J1122. Bold dots and lines represent the 5-epoch averaged flux densities and errors, respectively. Similarly, the grey dots and lines also represent the flux densities of the individual observations. Right panel: auroral ring model with a certain geometric configuration used to explain the radio lightcurves of J1122 [20].

A combination of the auroral ring model and radio observations can unveil important geometrical parameters such as the inclination of the rotation and magnetic axes, auroral ring colatitude, etc, some of which are inaccessible in these extremely cool objects otherwise. This method has been successfully applied for the first time very recently [21] and represents a robust new tool for studying magnetic fields on planetary-mass objects.

## Acknowledgments

The European VLBI Network is a joint facility of independent European, African, Asian, and North American radio astronomy institutes. J.B.C., J.C.G., and J.M.M. were supported by Ministerio de Ciencia e Innovación/ Agencia Estatal de Investigación (grants PGC2018-098915-B-C22 and PID2020-117404GB-C22). M.P.T. and L.P.M. were supported by Ministerio de Ciencia e Innovación (grants PID2020-117404GB-C21 and CEX2021-001131-S) and by the European Union (NextGenerationEU grant PRTR-C17.I1). J.B.C. and J.C.G. were supported by grants PROMETEO/2020-080, ASFAE/2022/018, and CIPROM/2022/64.

## References

- [1] Berger, E. et al. 2001, *Nature*, 410, 6826
- [2] Route & Wolszczan 2016, *ApLL*, 821, 2
- [3] Vedantham et al. 2020, *ApJL*, 903, 2
- [4] Vedantham et al. 2023, *A&A*, 675, L6
- [5] Williams et al. 2017, *ApJ*, 834, 117
- [6] Hallinan et al. 2006, *Apj*, 653, 1
- [7] Güdel 2002, *ARA&A*, 40, 217
- [8] Pineda et al. 2017, *ApJ*, 846, 1
- [9] Saur et al. 2021, *A&A*, 655, A75
- [10] Dulk 1985, *ARA&A*, 23, 169
- [11] Hallinan et al. 2008, *ApJ*, 684, 1
- [12] Güdel & Benz 1993, *ApJL*, 405, 63
- [13] Berger, E., Basri, G., et al. 2008, *ApJ*, 676, 2
- [14] Berger 2006, *ApJ*, 648, 1
- [15] Hallinan et al. 2015, *Nature*, 523, 7562
- [16] Metodieva et al. 2017, *MNRAS*, 465, 2
- [17] Miles-Páez, et al. 2023, *MNRAS*, 521, 952
- [18] Climent et al. 2023, *Science*, 381, 6662
- [19] Guirado et al. in prep
- [20] Bloot et al. 2024, *A&A*, 682A, 170
- [21] Kavanagh et al., arXiv:2410.18073